



HAL
open science

Insights into Cu₂O Thin Film Absorber via Pulsed Laser Deposition

Chithira Venugopalan Kartha, Jean Luc Rehspringer, Dominique Muller, Stéphane Roques, Jérémy Bartringer, Gerald Ferblantier, Abdelilah Slaoui, Thomas Fix

► **To cite this version:**

Chithira Venugopalan Kartha, Jean Luc Rehspringer, Dominique Muller, Stéphane Roques, Jérémy Bartringer, et al.. Insights into Cu₂O Thin Film Absorber via Pulsed Laser Deposition. *Ceramics International*, 2022, 48 (11), pp.15274-15281. 10.1016/j.ceramint.2022.02.061 . hal-03651711

HAL Id: hal-03651711

<https://hal.science/hal-03651711>

Submitted on 25 Apr 2022

HAL is a multi-disciplinary open access archive for the deposit and dissemination of scientific research documents, whether they are published or not. The documents may come from teaching and research institutions in France or abroad, or from public or private research centers.

L'archive ouverte pluridisciplinaire **HAL**, est destinée au dépôt et à la diffusion de documents scientifiques de niveau recherche, publiés ou non, émanant des établissements d'enseignement et de recherche français ou étrangers, des laboratoires publics ou privés.

Insights into Cu₂O Thin Film Absorber via Pulsed Laser Deposition

Chithira Venugopalan Kartha^{a}, Jean-Luc Rehspringer^b, Dominique Muller^a, Stéphane Roques^a, Jérémy Bartringer^a, Gérald Ferblantier^a, Abdelilah Slaoui^a, Thomas Fix^a*

^a Icube Laboratory, Université de Strasbourg and CNRS, 23 rue du Loess, BP 20 CR, F-67037 Cedex 2 Strasbourg, France

^b Institut de Physique et Chimie des Matériaux de Strasbourg (IPCMS), UMR 7504 CNRS and Université de Strasbourg, 23 rue du Loess, BP43, F-67034 Cedex 2 Strasbourg, France

*Corresponding Author

*Email: venugopalan@unistra.fr

ABSTRACT: Cuprous oxide materials are of growing interest for optoelectronic devices and were produced by several chemical and physical methods. Here, we report on the structural, optical, and electrical properties of Cu_xO thin films prepared by the pulsed laser deposition technique. The substrate temperature, as well as the oxygen partial pressure in the deposition chamber, were varied to monitor the copper to oxygen ratio within the deposited films. The growth conditions were carefully optimized to provide the highest conductivity and mobility. Thus, 100 nm thick cuprous oxide films (Cu_2O) deposited at 750 °C exhibited a resistivity of 16 $\Omega\cdot\text{cm}$, high mobility of 30 $\text{cm}^2/(\text{V}\cdot\text{s})$, and a bandgap of around 2 eV. The film deposited at the optimized deposition parameters on Nb:STO (001) substrate with Au top electrode showed a photovoltaic response with an open circuit voltage of 0.56 V. These results path the way to efficient solar cells made with Cu_2O films via the pulsed laser deposition technique.

KEYWORDS: Pulsed Laser Deposition, Cu_2O , CuO, Absorber, Solar Cell, Rutherford Backscattering

1.INTRODUCTION

Among thin film absorbing oxides, Cu_2O is the most popular and is widely studied for optoelectronic and photovoltaic applications [1]. As it is non-toxic, abundant, and low cost, it greatly fulfills the economic and environmental conditions for large-scale applications [2]. Cu_2O is an inherently p-type semiconductor with a direct bandgap of 2.17 eV [3] and high absorption coefficient of above 10^5 cm^{-1} in the visible region of the solar spectrum [4] which makes it a potential candidate as absorbers in solar cells. However, the highest practical efficiency of a solar cell with a Cu_2O absorber achieved so far is only 8.1 % [5] even though the theoretical efficiency is around 18 % when referring to the Shockley-Queisser limit [6]. Hence, there is immense potential for improvement in the structural and charge transport properties.

In the literature, there are numerous preparation methods for Cu₂O thin films, which include both chemical [7–9] and physical processes [10–12]. Few of the most commonly followed techniques include electrodeposition [13–15], thermal oxidation [16–18], magnetron sputtering [19–21] and, atomic layer deposition (ALD) [22–24]. Pulsed laser deposition (PLD) is another physical technique for high quality film deposition. However, there are very few works on Cu₂O deposition by PLD [25–32] as it is very difficult to reach the correct phase for the films due to the deposition at non-equilibrium conditions. Nevertheless, the properties of the PLD deposited films highly depend on the deposition parameters such as laser fluence, background gas, substrate temperature, the distance between target and substrate which allow for better control of the film properties which can be manipulated for various applications. Thermodynamic conditions play a strong influence on the Cu-O phase formed via PLD [33]. Chen et.al [26] and Liu et.al [30] have shown that an increase in chamber pressure changes plasma dynamics from the ballistic to diffuse regimes, which results in different Cu-O phases. Chen et al also show the influence of temperature, wherein they mention that at 4×10^{-4} mbar pressure, a variation in temperature between 400-700 °C changes the orientation of the films. Moreover, they showed that mixed films of CuO and Cu₂O are obtained at higher pressures above 1×10^{-3} mbar and CuO films are formed above 4×10^{-2} mbar. However, Jawad et al [29] claim that films deposited at a fixed oxygen partial pressure of 10^{-3} mbar and different temperatures allow the control of the film's phase between CuO and Cu₂O. Subramaniyan et.al [34] have managed to obtain phase pure Cu₂O at 3×10^{-4} mbar oxygen partial pressure and temperature in the range of 308-325 °C where CuO is the equilibrium phase, by varying the total chamber pressure which they explain to have a non-monotonic effect on Cu-O formation. Later, Farhad et.al [35] claim to have obtained p-type films at room temperature at an oxygen partial pressure of $2-3 \times 10^{-3}$ mbar. The inherent p-type conductivity of Cu₂O film originates from copper vacancies in the crystal lattices [36,37]. Even though there are few reports on undoped n-type Cu₂O

thin films from electrodeposition [38–40] and PLD [29,41], which claim oxygen vacancies and copper interstitial defects as the donor sources, it is still a matter of debate [42].

In this work, we have proven that better control of the film stoichiometry can be achieved by controlling the oxygen partial pressure and temperature during pulsed laser deposition. On the other hand, while all the previous investigations on the influence of temperature and oxygen partial pressure on the Cu_xO_y films in the literature are based on very local small scale evaluation on the stoichiometry, in this paper we present a detailed analysis using Rutherford Backscattering Spectroscopy (RBS) for the evaluation of stoichiometry in the range of 1 mm^2 area. Additional characterization techniques were carried out to further confirm the findings. Subsequently, we have managed to find the correct Cu_2O phase at both low temperature and high temperature which opens up the possibility of using these films for applications without the limitation of deposition temperature. The potential of using the Cu_2O film as an absorber is also discussed in this work.

2. EXPERIMENTAL SECTION

The Cu_xO films were deposited in a PLD chamber using a CuO target. 5 mg CuO powder was pressed into a pellet and later sintered at $900 \text{ }^\circ\text{C}$ for 1 hour to make the target. The deposition was carried out using a KrF excimer laser at a repetition rate of 10 Hz with $1\text{-}2 \text{ J/cm}^2$ laser fluence on the target. The target-substrate distance was fixed at 55 mm. Most of the films were deposited on $10 \times 10 \text{ mm}^2$ quartz substrates. After the deposition, the samples were cooled down naturally under the same oxygen partial pressure used for deposition. Films were prepared at a range of temperatures from room temperature up to $800 \text{ }^\circ\text{C}$ at oxygen partial pressures of 10^{-2} and 10^{-3} mbar for a detailed study of the film composition and properties. For a better understanding of the influence of temperature and oxygen partial pressure for the controlled growth of Cu_2O and CuO films, the results of four samples are discussed in more detail. Experimental conditions of their

growth are given in **Table 1**. In order to study the application of the Cu₂O film as an absorber, a 100 nm thin film was deposited at 750 °C and 10⁻² mbar on a commercially bought 1x1 cm² Nb (1 at%) doped SrTiO₃ (STO) (001) substrate (resistivity of 0.01 Ω·cm). Nb doped STO is a crystalline conductive substrate which is an n-type semiconducting oxide. On the Cu₂O layer deposited on Nb:STO, a 7 nm thick semi-transparent gold (Au) film is deposited as the top electrode by Thermal Evaporation through a 1 mm² steel mask resulting in a solar cell with the architecture Nb:STO (001)// Cu₂O/Au.

Table 1. Experimental Details of Samples

Sample	Temperature	Oxygen Partial Pressure
A	750 °C	10 ⁻² mbar
B	300 °C	10 ⁻³ mbar
C	650 °C	10 ⁻³ mbar
D	200 °C	10 ⁻² mbar

The atomic composition and thickness of the deposited films under different temperatures and oxygen partial pressure were studied in detail by Rutherford Backscattering Spectroscopy (RBS) using-1.5 MeV He⁺ particles from the Van de Graaff accelerator (HVEE KN4000) facility at ICube. The samples were tilted at an angle of 45 degrees for all the measurements. For completeness on films composition, a Horiba LabRAM ARAMIS Raman spectrometer with 532 nm laser excitation was used to study the Raman footprints of the deposited films. On the other hand, the crystallographic properties of the deposited films were carried out thanks to X-ray diffraction studies using a Rigaku Smartlab diffractometer equipped with a monochromatic source delivering a Cu Kα₁ incident beam (45 kV, 200 mA, 0.154056 nm) and Bruker-AXS D8 Advance X-ray

diffractometer with $\text{CuK}\alpha_1$ radiation ($\lambda = 0.154056$ nm). The morphology of the PLD films were analyzed by scanning electron microscopy performed using a Gemini 500-Zeiss apparatus. The roughness of the Cu_2O films was found out using a NT-MDT SMENA Atomic Force Microscope. Optical characterization of the samples was carried out using a Horiba Uvisel Lt M200 FGMS (210-880 nm) spectroscopic ellipsometer. Photoluminescence measurements were carried out using a 532 nm HeNe laser of 100 mW output. The work function of the samples was determined using a single point Kelvin Probe from KP Technology (KP020) with a resolution of 1-3 meV. The electrical properties were analyzed using a four-point probe measurement by an Ecopia Hall effect measurement system (HMS-5000) at room temperature. The I-V properties of the solar cell were obtained using an AAA rated ORIEL Verasol-2 LED Solar Simulator (LSS-7120) and a Keithley 2461 Source Measure Unit.

3.RESULTS AND DISCUSSION

The stoichiometry of the thin films deposited at different temperatures and oxygen partial pressures were determined from RBS analysis. The spot size of RBS analysis being 1 mm^2 allows for a better understanding of the film composition than any other local characterization technique. RBS spectra can be also used for thickness determination and elemental analysis. Since the oxygen concentration is proportionate to copper, the elemental composition of O from the RBS analysis is calculated with respect to copper concentration. The error for this measurement depends on the quality of the film and a maximum of 10-15 % error can be expected. The height of the peak plateau in an RBS spectrum (**Figure S1**) gives the copper concentration and the width of the peak provides the thickness of the film. The thicknesses of all the films used in this study were estimated from RBS analysis. The films used for comparing the properties henceforth in this paper are all approximately 100 nm from RBS estimation.

Figure 1 shows the oxygen concentration variation with respect to copper in Cu_xO as determined from the RBS spectra using the SAM tool [43]. The films were found to be very sensitive to the temperature of the deposition and the oxygen partial pressure. Similar to the findings of Wee et.al [28] it was observed that the Cu_2O phase without any trace of the CuO is only possible in a limited deposition window of oxygen partial pressure and temperature. The thin films prepared at the same temperature but at different pressures are found to be stoichiometrically different. At a higher oxygen partial pressure of 10^{-2} mbar and a higher temperature of $750\text{ }^\circ\text{C}$ (sample A in **Figure 1**), the film has 0.5 oxygen concentration which corresponds to Cu_2O . Among the three samples prepared under the same conditions, two of them showed identical oxygen to copper ratio whilst for the third sample, deviation of ratio to 0.75 could be attributed to the variation in the time of preparation of the sample wherein additional factors such as changes in the pumping system and laser alignment might have influenced the phase of the sample. Sample C prepared at a higher temperature range with a lower oxygen pressure of 10^{-3} mbar has a concentration of 0.9 which is close to CuO . However, for a low-temperature range of deposition ($200\text{-}300\text{ }^\circ\text{C}$), oxygen partial pressure of 10^{-3} mbar is favorable for Cu_2O deposition as can be seen when the samples B and D are compared in **Figure 1**. At lower temperatures, a higher amount of oxygen results in the formation of CuO . However, the reason that the same trend is not observed at higher temperatures could be because, as explained by Sambri et.al [44], the increase in substrate temperature during deposition reduces the background gas resistance thus changing the background gas density within the chamber, hence apart from the thermal effect on the surface kinetics, they also influence the precursors in the gas phase. At a higher partial pressure of 10^{-2} mbar, it was observed in this work that the films are highly sensitive to the temperature as there was variation in the copper to oxygen ratio for even $25\text{ }^\circ\text{C}$ variations of temperature (between $700\text{-}750\text{ }^\circ\text{C}$ in **Figure 1**). This behavior, which was confirmed by repeating the sample twice could be also because of the change in the

background gas density with temperature. Unlike the observation of Farhad et.al [28], here the films deposited at room temperature under both pressure conditions resulted in the CuO phase.

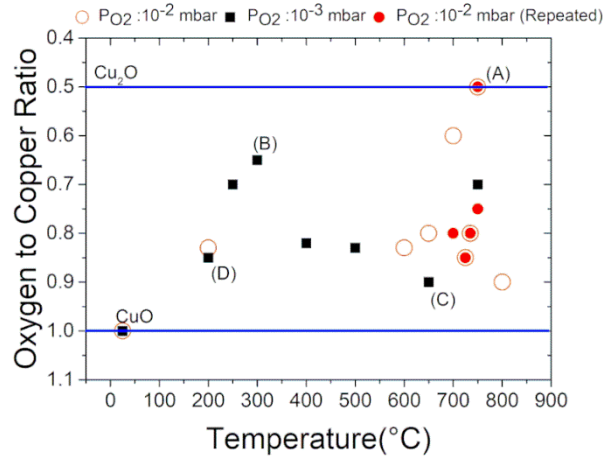


Figure 1. Oxygen to copper ratio in Cu_xO v.s temperature at 10^{-2} mbar and 10^{-3} mbar oxygen partial pressures (estimated from RBS measurements).

Raman spectroscopic analysis of all the samples showed a similar phase as from the stoichiometry analysis from RBS. RRUFF is a digitalization project which provides free access to approximately 3,500 mineral spectra [45]. The Raman spectra in this work are compared with the spectra in the RRUFF reference database using 532 nm laser excitation. Hence the peak positions are based on similar conditions in the reference and experimental spectra. The vibrational modes of Cu_2O were observed in both samples A and B as can be seen in **Figure 2**. T_{1u} mode, second-order E_u ($2E_u$) mode, and multi phonon process (MPP) mode were observed at 145 cm^{-1} , 216 cm^{-1} , and 412 cm^{-1} respectively similar to the Cu_2O reference (RRUFF reference: R140763). The T_{1u} mode corresponds to phonons activated by defects namely copper vacancies and copper interstitials from which the p-type conductivity of Cu_2O originates [46]. As the intensity ratio of peaks at 145 cm^{-1} (T_{1u}) and 216 cm^{-1} ($2E_u$) is sensitive to surface damages [47], comparing samples A and B, sample B might have more surface damages. On the other hand, samples C and D show Raman peaks at 274 cm^{-1} and 287 cm^{-1} respectively, which is close to the characteristic Raman peak of CuO at

297 cm^{-1} according to the RRUFF reference (R120076) of CuO. Such data confirm the RBS results of the film stoichiometry.

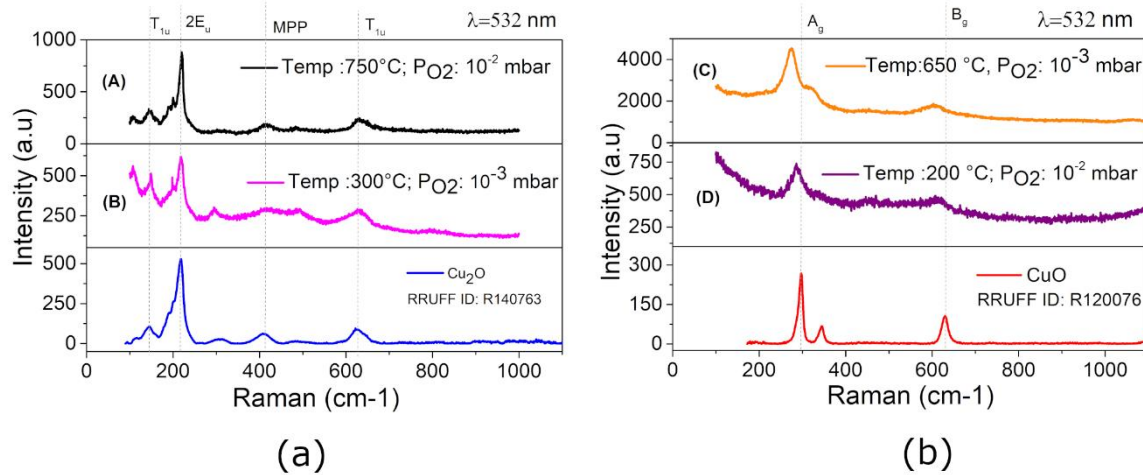


Figure 2. Raman spectra of (a) A and B (b) C and D deposited at different temperatures and oxygen partial pressures on quartz along with the references from RRUFF database translated for viewing purpose (excitation wavelength = 532 nm).

X-ray diffraction analyses were carried out on the four selected samples as they represent the various configurations of the PLD grown Cu_xO films. The results are plotted in **Figure 3** and they all show good crystallization of the films. Sample B is less crystalline than sample A. Sample A has preferred orientation in (2 0 0) direction, unlike the reference. The X-ray spectra of sample A and B at a grazing angle of 3° exhibit significant Cu₂O peaks for (2 0 0), (3 1 1), (2 2 0), and (1 1 1) while sample D showed only CuO peaks of (-1 1 1) and (1 1 1). However, unlike the results from RBS and Raman analysis, sample C has a Cu₂O peak of (1 1 1) which could result from a mix of Cu₂O and CuO composition within the sample and XRD being a large surface analysis technique compared to RBS might have focused on the area of Cu₂O. The lattice parameters of the samples were calculated from the XRD peaks and the values for Sample A and B which showed Cu₂O stoichiometry are listed in **Table 2**. The mean grain size of the crystallites was calculated using

the Scherrer equation [48]. Sample A is found to have larger grain size (15.1 ± 0.6 nm) than all the four samples. The grain size shows a decreasing trend with temperature comparing Sample A and Sample D (10.4 ± 0.9 nm). The higher full width half maximum of the prominent peaks in Sample B over sample A could be an indication of lattice strain, point defects, dislocations in the material apart from instrumental effects. The microstrain calculated in sample B deposited at lower temperature using Stokes –Wilson relation [49] is found to be double than that in sample A. Similarly, the lattice constant calculated of sample A is same as pure Cu_2O (4.267 \AA from JCPDS: 01-078-2076) whereas there is an approximately 0.5% deviation for sample B which could be an indication of lattice strain. The stress in the films was calculated from the measured lattice constant using the equation $\sigma = (-E (a-a_0))/2va_0$ [50,51]. Sample A is found to have a very low tensile stress of 0.01 GPa whereas sample B had tensile stress of 0.22 GPa. Sample D have a compressive stress of 0.57 GPa. The d-spacing of sample A are expected values for the dominant peaks of pure Cu_2O film and a slight deviation was observed for sample B as expected. Detailed study on all the parameters points to sample A deposited at $700 \text{ }^\circ\text{C}$, 10^{-2} mbar to be of better quality film.

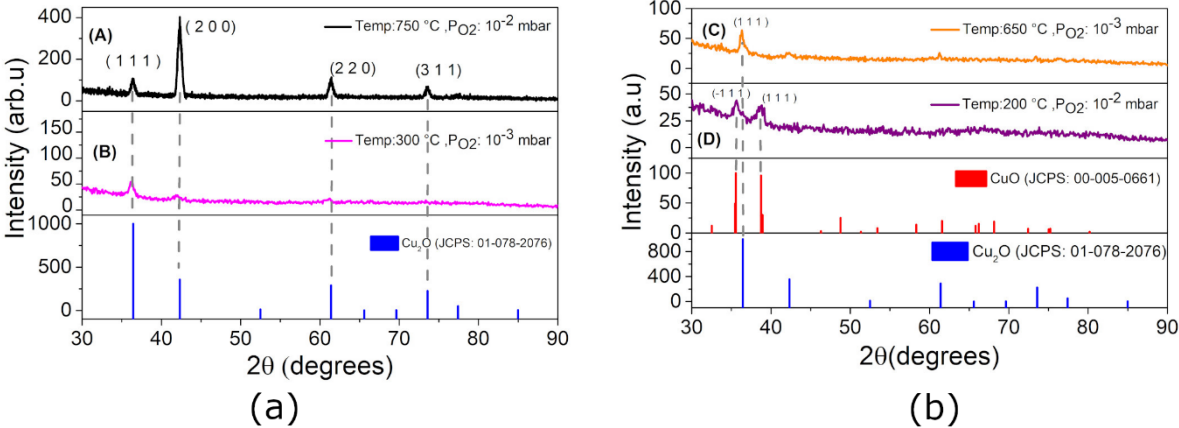


Figure 3. Grazing angle X-ray diffraction ($\text{CuK}\alpha_1$ radiation ($\lambda = 0.154056 \text{ nm}$)) pattern of (a) A and B (b) C and D on quartz and reference of Cu_2O and CuO from the ICCD database.

Table 2. Lattice Parameters, Crystallites Sizes and Micro strain of Samples A and B calculated from the X-ray diffraction peaks

Sample	2θ ($^\circ$)	FWHM ($^\circ$)	d spacing (\AA)	Micro strain	Mean Grain Size (nm)	Lattice Constant (\AA)
(A)	36.39	0.57	2.46	7.56	14.69	4.27
	42.31	0.59	2.13	6.63	14.48	4.27
	61.38	0.59	1.51	4.39	15.48	4.27
	73.56	0.63	1.29	3.66	15.79	4.27
(B)	36.23	0.63	2.47	8.41	13.25	4.29
	41.93	1.41	2.15	16.08	6.02	4.30
	61.01	0.91	1.52	6.71	10.18	4.29

The optical properties of the Cu_xO films are of interest for optoelectronic applications. The absorption coefficient from ellipsometry data is depicted in **Figure 4**. The dispersion models used for Cu_2O and CuO are the Triple Tauc Lorentz and simple Tauc Lorentz formulas respectively [52]. The figure of merit related to χ -squared values was below 0.6 for Cu_2O samples. Both the Cu_2O samples (samples A and B) have a high absorption coefficient in the range of 10^5 cm^{-1} in the visible region. For sample A, deposited at $750 \text{ }^\circ\text{C}$, 10^{-2} mbar , the peak of yellow exciton transition at 560 nm (E_{OA} edge) and 2D exciton transitions at 349 nm ($E_{1\text{A}}$) and at 290 nm ($E_{1\text{B}}$) is visible which is similar to that of Cu_2O in literature [53]. However, for Sample B ($300 \text{ }^\circ\text{C}$, 10^{-3} mbar) apart from the 2D exciton transitions, the indigo exciton peak (E_{OD} edge) at 440 nm is visible. As the symmetry

of the CuO crystal is low compared to Cu₂O, the spectra of CuO do not have sharp structures. Similar behavior is shown by samples C and D. The absorption coefficient peak is from E₄ transition at 315 nm which is similar to CuO [54].

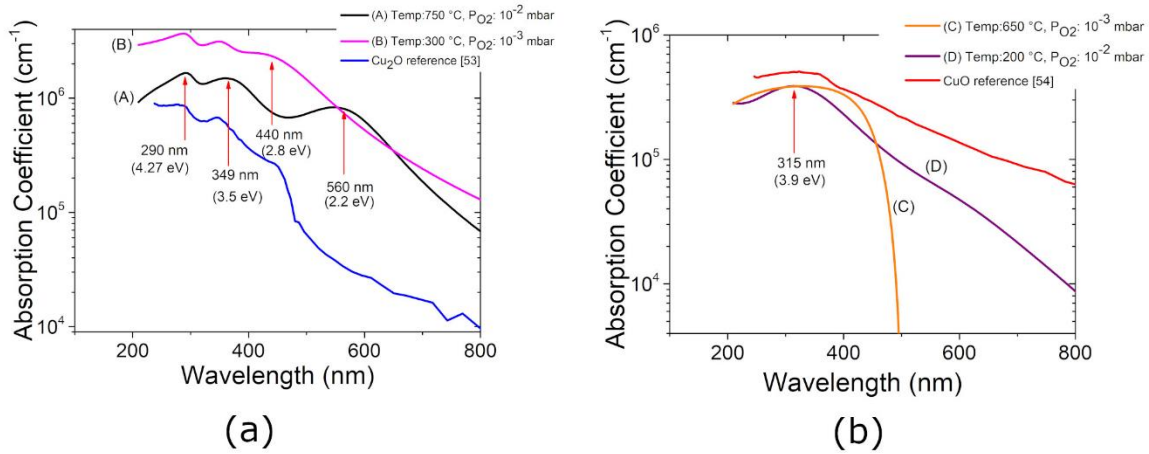


Figure 4. Variation of absorption coefficient v.s wavelength of (a) A, B (b) C and D deposited at different temperatures and pressures on quartz.

For the use of a thin film as an absorber, having a high carrier concentration without compromising the mobility is very essential. The electrical properties of the samples A, B, C, and D obtained from the hall measurement are listed in **Table 3**. All the Cu₂O films reported here are p-type with a Hall concentration in the range of 10¹⁵ cm⁻³, which is consistent with the Cu₂O films prepared via other techniques [3,55,56]. In particular, it should be noticed that sample A (deposited at 750 °C and 10⁻² mbar oxygen partial pressure) could demonstrate a resistivity as low as 16 Ω·cm and high mobility of 30 cm²/(V·s) at room temperature. Comparison of the electrical properties of this Cu₂O film (sample A deposited at 750 °C and 10⁻² mbar oxygen partial pressure) to films prepared via different growth techniques is outlined in **Table 4**. The bulk concentration and resistivity of the PLD film in this work are comparable to high-temperature PLD deposited Cu₂O from literature. Also when compared to other popular techniques for Cu₂O preparation, the film in this work have

low resistivity and also bulk concentration in the range required for device applications [31]. Sample A showed higher mobility without deteriorating the carrier concentration than most of the films via PLD reported in the literature [28,30]. To the best of our knowledge, all the previous work which have reported high mobility without compromising the carrier concentration was on single-crystal substrates. Further, the work function of sample A from Kelvin probe measurements is 4.98 eV which is similar to the literature for Cu₂O film [57,58]. In contrast, sample B deposited at lower temperature and oxygen partial pressure exhibits a higher resistivity and lower mobility compared to sample A that could be because of the poor film quality which will be discussed later. The bandgap of the films is calculated from the Tauc plot ($h\nu$ vs $(\alpha h\nu)^{1/r}$) assuming that Cu₂O have direct forbidden transitions and thus using the exponent $r=3/2$ [59,60] and for the CuO films, $r=2$ considering they have indirect bandgap [53]. Samples A and B have a bandgap of 1.8-2.1 eV which corresponds to Cu₂O from literature. For CuO films the bandgap varies from 1.2-2.6 eV depending on the preparation conditions [61]. The samples C and D have a bandgap which is close to the CuO film via PLD in literature [62].

Table 3. Electrical properties and work function of the PLD deposited films

Sample	Composition (from RBS Estimation)	Temperature (°C)	Oxygen Partial Pressure (mbar)	Resistivity ($\Omega\cdot\text{cm}$)	Bulk concentration (cm^{-3})	Mobility ($\text{cm}^2/(\text{V}\cdot\text{s})$)	Work function (eV)	Bandgap (ev)
(A)	Cu ₂ O	750	10 ⁻²	40.0±24.0	+5.0x10 ¹⁵ ±4.0x10 ¹⁵	22.5±8.5	4.98	2.05±0.05
(B)	Cu ₂ O	300	10 ⁻³	329.0±0.8	+2.4x10 ¹⁵ ±1.0x10 ¹⁵	9.0±0.2	5.17	1.80±0.10
(C)	CuO	650	10 ⁻³	161.0±53.0	+2.3x10 ¹⁵ ±8.4x10 ¹⁵	18.0±1.5	5.07	1.92±0.20
(D)	CuO	200	10 ⁻²	2600.0±100.0	+4.0x10 ¹⁴ ±1.3x10 ¹⁴	4.8±3.7	5.21	1.85±0.10

Table 4. Electrical properties of the Cu₂O film via different techniques

Type of Preparation	Resistivity ($\Omega\cdot\text{cm}$)	Mobility ($\text{cm}^2/(\text{V}\cdot\text{s})$)	Bulk concentration (cm^{-3})	Reference
PLD	16-64	14.0-31.0	1.0×10^{15} – 9×10^{15}	This work
PLD	60	26	1×10^{13} – 1×10^{16}	[31,33,63]
Sputtering (RF)	2×10^{-1} - 4×10^{-2}	0.08-2.23	5.8×10^{18} – 2.1×10^{21}	[64]
Thermal Oxidation	1×10^3	100.00	1.0×10^{13} – 1.0×10^{14}	[65]
Electrodeposition	2.7×10^4 - 3.3×10^6	0.4-1.8	10^{12} - 10^{14}	[66]
ALD	64-160	42-92	2×10^{15} - 7×10^{15}	[24]

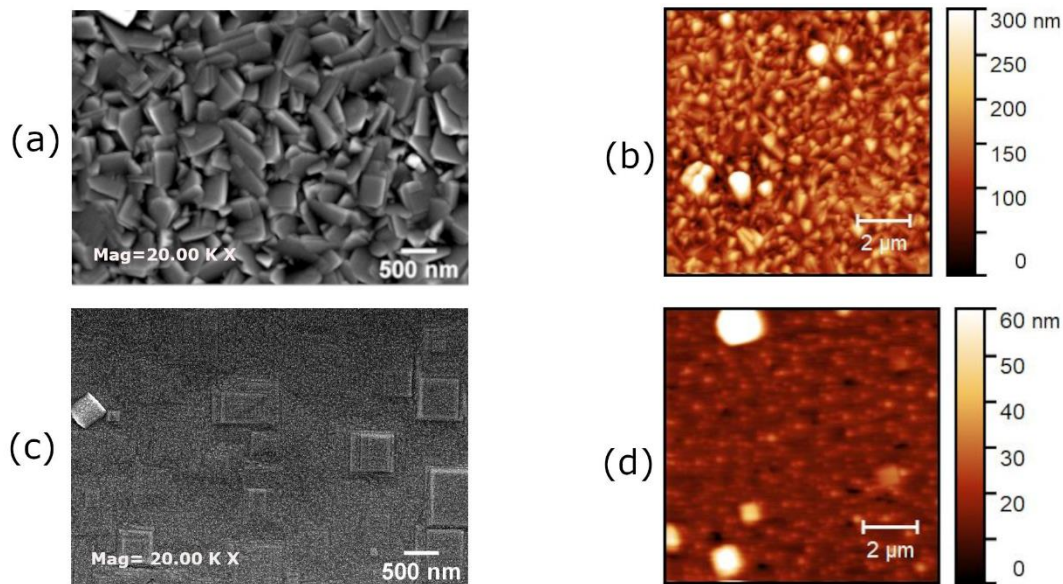


Figure 5. (a) Secondary electron image (b) AFM image of sample A deposited at 750 °C, 10^{-2} mbar on quartz (c) Secondary electron image (d) AFM image of sample deposited at similar conditions as sample A on Nb:STO (001). The squares in the Nb:STO//Cu₂O samples are STO outgrowths.

The scanning electron microscopy (SEM) applied to sample A (750°C, 10^{-2} mbar) confirms that the morphological structure of the Cu₂O film is polycrystalline (**Figure 5(a)**). The SEM image also shows rectangular shaped grains with rather uniform coverage with very much fewer holes which are preferable for photovoltaic applications. The higher grain size observed in SEM compared to the calculated values from the diffraction peaks is an indication that the diffraction peak broadening

might be due to defects and stress in the material and not just due to the influence of grain size. However, the secondary electron image of sample B revealed that the low temperature deposited Cu_2O film has more flat morphology with smaller grains (**Figure S2(a)**). A similar change in surface morphology with temperature was also observed by Subramaniyan et.al [34]. The roughness analysis by AFM of sample A (**Figure 5 (b)**) revealed a higher RMS roughness of 47 nm but only 7 nm for sample B (**Figure S2(b)**) deposited at low temperature. Unlike sample A, sample B has the presence of holes and splashing which can affect the film properties during its application as an absorber, which agrees with the hint of surface damages revealed from the Raman spectra. Splashing arise from accumulations of ions which can be seen as the brightest points in the AFM image. These accumulations can create short-circuits when used in a solar cell.

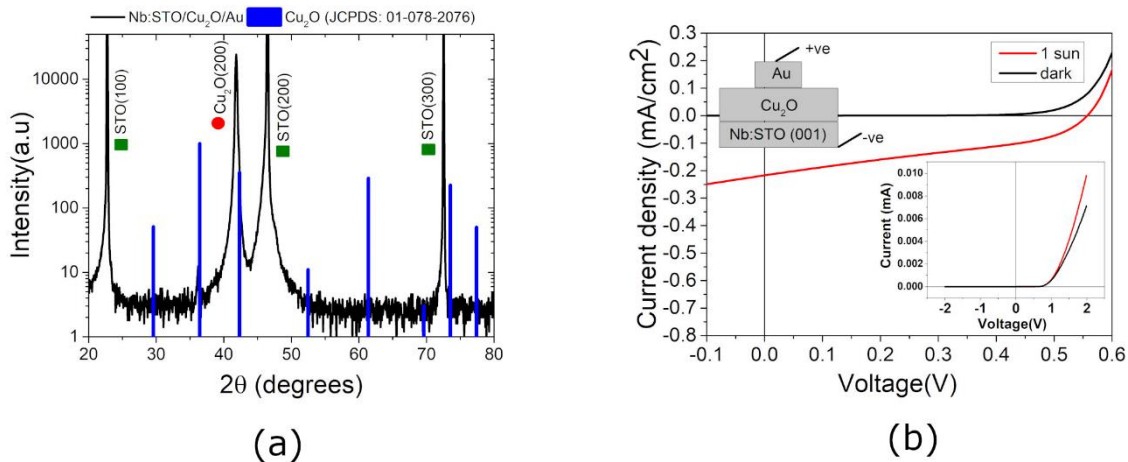


Figure 6. (a) θ - 2θ XRD diffractogram of (0 0 1) oriented Nb:STO // Cu_2O (100 nm)/Au(7 nm) (b) Corresponding current density vs voltage measured in dark and under 1 sun. A schematics of the solar cell structure is represented in the inset of (b).

In order to check the photovoltaic properties of our films, PLD of p-type Cu_2O layers deposited at 750 °C and 10^{-2} mbar was carried out on a crystalline and conductive substrate, namely Nb doped $\text{SrTiO}_3(001)$ sheets. **Figure 5(c)** shows the secondary electron image of the Cu_2O layer on Nb:STO

with uniform coverage and the AFM analysis revealed an RMS roughness of 15 nm. **Figure 6(a)** plots the X-ray diffraction spectra of Cu₂O/Nb:STO (001) exhibiting a single peak at (200) confirming the epitaxial growth. Even though the theoretical lattice mismatch between Cu₂O and Nb:STO is 8.5 % , a cube-on-cube epitaxial (Cu₂O (100) // STO (100)) relationship of Cu₂O and STO results in heteroepitaxial growth of the film on the substrate [32,67]. The peaks at $2\theta=22.7^\circ$, 46.5° , and 72.5° are from STO (100), STO (200), and STO (300) respectively. Nb:STO is the n-type semiconducting oxide contributing the p-n junction [32,68]. As the top electrode of the cell structure, an ultrathin gold layer, 7 nm thick, was evaporated making it semi-transparent with a transmission of 58% at 550 nm wavelength. **Figure 6(b)** shows the current-voltage characteristics of the solar cell measured in dark and light conditions using a solar simulator at 1 sun under AM 1.5 G conditions and a schematics of the solar cell structure is represented in the inset. The film exhibited a photovoltaic effect with a quite low short circuit current density of 0.21 mA/cm² but an open circuit voltage of 0.56 V. The open circuit voltage originates from the built in electric field which causes a built-in potential V_{bi} at the semiconductor heterojunction of Cu₂O and Nb:STO [32,69]. Apart from the low thickness of Cu₂O and absorption of the top electrode, the low current could be due to heterojunction defects or Cu₂O defects which require further advanced characterization and detailed studies. The solar cell had an efficiency of 0.053% and a fill factor of 45 %. It should be noted that the top Au layer is reducing the efficiency by a factor of ~ 2, additionally the non-optimal Cu₂O thickness (100 nm instead of 1000 nm) reduces the efficiency by a factor of 10. Thus a 20 times increase in the efficiency results in values comparable to optimized Cu₂O via PLD [32] even though the efficiency value is lower compared to solar cells with Cu₂O prepared via other popular techniques such as thermal oxidation [18] and electrodeposition [70]. A solar cell with similar architecture using low temperature Cu₂O as absorber (sample B) was also tested for comparison. However, the short circuit current density was

very low in the range of $\mu\text{A}/\text{cm}^2$ which could be due to the surface damages, the increased resistance, and low mobility of the film compared to sample A. Improvements in the heterojunction of the Cu_2O film also has huge potential in improving the photovoltaic parameters of Cu_2O absorber solar cells.

4. SUMMARY

Cu_2O films were successfully prepared using the pulsed laser deposition technique and by carefully optimizing oxygen partial pressure in the chamber and substrate deposition temperature. The variation in the chemical composition of the film and structural properties of the film were studied in detail using Rutherford Backscattering Spectroscopy, Raman spectroscopy, and X-ray diffraction techniques. The optical and electrical properties of the film deposited at $750\text{ }^\circ\text{C}$ and 10^{-2} mbar were found to be suited for the use as an absorber. The solar cell with the best film as an absorber with an architecture of Nb:STO (001)/ $\text{Cu}_2\text{O}/\text{Au}$ has a short circuit current density of $0.21\text{ mA}/\text{cm}^2$ and an open circuit voltage of 0.56 V . This work provides insights into the potential of pulsed laser deposition of cuprous oxide films and its potential application as an absorber.

ASSOCIATED CONTENT

Supporting Information: RBS yield of Cu_2O ; SEM and AFM image of low temperature deposited Cu_2O .

FUNDING

This work was supported by Centre National de la Recherche Scientifique (CNRS) and University of Strasbourg.

AUTHOR INFORMATION

Corresponding Author

Chithira Venugopalan Kartha

venugopalan@unistra.fr

ACKNOWLEDGEMENTS

The authors would like to acknowledge the contribution of C. Leuvre and M. Lenertz from the Institut de Physique et Chimie des Matériaux de Strasbourg (IPCMS) for the scanning electron microscopy and XRD analysis respectively. The authors also wish to thank the staff from the C³FAB platform of ICube laboratory.

REFERENCES

- [1] M. Coll, J. Fontcuberta, M. Althammer, M. Bibes, H. Boschker, A. Calleja, G. Cheng, M. Cuoco, R. Dittmann, B. Dkhil, I. El Baggari, M. Fanciulli, I. Fina, E. Fortunato, C. Frontera, S. Fujita, V. Garcia, S.T.B. Goennenwein, C.-G. Granqvist, J. Grollier, R. Gross, A. Hagfeldt, G. Herranz, K. Hono, E. Houwman, M. Huijben, A. Kalaboukhov, D.J. Keeble, G. Koster, L.F. Kourkoutis, J. Levy, M. Lira-Cantu, J.L. MacManus-Driscoll, J. Mannhart, R. Martins, S. Menzel, T. Mikolajick, M. Napari, M.D. Nguyen, G. Niklasson, C. Paillard, S. Panigrahi, G. Rijnders, F. Sánchez, P. Sanchis, S. Sanna, D.G. Schlom, U. Schroeder, K.M. Shen, A. Siemon, M. Spreitzer, H. Sukegawa, R. Tamayo, J. van den Brink, N. Pryds, F.M. Granozio, Towards Oxide Electronics: a Roadmap, *Applied Surface Science*. 482 (2019) 1–93. <https://doi.org/10.1016/j.apsusc.2019.03.312>.
- [2] A.E. Rakhshani, Preparation, characteristics and photovoltaic properties of cuprous oxide—a review, *Solid-State Electronics*. 29 (1986) 7–17. [https://doi.org/10.1016/0038-1101\(86\)90191-7](https://doi.org/10.1016/0038-1101(86)90191-7).
- [3] Ø. Nordseth, I. Chilibon, B.G. Svensson, R. Kumar, S.E. Foss, C. Vasiliu, L. Baschir, D. Savastru, L. Fara, C. Dumitru, S. Fara, F. Dragan, M. Filipescu, R. Trusca, Characterization of Cuprous Oxide Thin Films for Application in Solar Cells, *DF*. 22 (2019) 65–73. <https://doi.org/10.4028/www.scientific.net/DF.22.65>.
- [4] C. Malerba, F. Biccari, C. Leonor Azanza Ricardo, M. D’Incau, P. Scardi, A. Mittiga, Absorption coefficient of bulk and thin film Cu₂O, *Solar Energy Materials and Solar Cells*. 95 (2011) 2848–2854. <https://doi.org/10.1016/j.solmat.2011.05.047>.
- [5] T. Minami, Y. Nishi, T. Miyata, Efficiency enhancement using a Zn_{1-x}Ge_x-O thin film as an n-type window layer in Cu₂O-based heterojunction solar cells, *Appl. Phys. Express*. 9 (2016) 052301. <https://doi.org/10.7567/APEX.9.052301>.
- [6] W. Shockley, H.J. Queisser, Detailed Balance Limit of Efficiency of p-n Junction Solar Cells, *Journal of Applied Physics*. 32 (1961) 510–519. <https://doi.org/10.1063/1.1736034>.
- [7] M. Ristov, G. Sinadinovski, I. Grozdanov, Chemical deposition of Cu₂O thin films, *Thin Solid Films*. 123 (1985) 63–67. [https://doi.org/10.1016/0040-6090\(85\)90041-0](https://doi.org/10.1016/0040-6090(85)90041-0).
- [8] N. Saadaldin, M.N. Alsloom, N. Hussain, Preparing of Copper Oxides Thin Films by Chemical Bath Deposition (CBD) for Using in Environmental Application, *Energy Procedia*. 74 (2015) 1459–1465. <https://doi.org/10.1016/j.egypro.2015.07.794>.

- [9] A.B. Laurie, M.L. Norton, Preparation and characterization of thin films of copper(II) oxide by low temperature normal pressure metalorganic chemical vapor deposition, *Materials Research Bulletin*. 24 (1989) 213–219. [https://doi.org/10.1016/0025-5408\(89\)90128-1](https://doi.org/10.1016/0025-5408(89)90128-1).
- [10] D. Chua, S.B. Kim, K. Li, R. Gordon, Low Temperature Chemical Vapor Deposition of Cuprous Oxide Thin Films Using a Copper(I) Amidinate Precursor, *ACS Appl. Energy Mater.* 2 (2019) 7750–7756. <https://doi.org/10.1021/acsaem.9b01683>.
- [11] N. Gupta, R. Singh, F. Wu, J. Narayan, C. McMillen, G.F. Alapatt, K.F. Poole, S.-J. Hwu, D. Sulejmanovic, M. Young, G. Teeter, H.S. Ullal, Deposition and characterization of nanostructured Cu₂O thin-film for potential photovoltaic applications, *Journal of Materials Research*. 28 (2013) 1740–1746. <https://doi.org/10.1557/jmr.2013.150>.
- [12] T. Iivonen, M.J. Heikkilä, G. Popov, H.-E. Nieminen, M. Kaipio, M. Kemell, M. Mattinen, K. Meinander, K. Mizohata, J. Räisänen, M. Ritala, M. Leskelä, Atomic Layer Deposition of Photoconductive Cu₂O Thin Films, *ACS Omega*. 4 (2019) 11205–11214. <https://doi.org/10.1021/acsomega.9b01351>.
- [13] Y. Tolstova, S.S. Wilson, S.T. Omelchenko, N.S. Lewis, H.A. Atwater, Molecular Beam Epitaxy of Cu₂O Heterostructures for Photovoltaics, in: 2015 IEEE 42nd Photovoltaic Specialist Conference (PVSC), 2015: pp. 1–4. <https://doi.org/10.1109/PVSC.2015.7355913>.
- [14] I.S. Brandt, M.A. Tumelero, S. Pelegrini, G. Zangari, A.A. Pasa, Electrodeposition of Cu₂O: growth, properties, and applications, *Journal of Solid State Electrochemistry*. 21 (2017) 1999–2020. <https://doi.org/10.1007/s10008-017-3660-x>.
- [15] M. Balik, V. Bulut, I.Y. Erdogan, Optical, structural and phase transition properties of Cu₂O, CuO and Cu₂O/CuO: Their photoelectrochemical sensor applications, *International Journal of Hydrogen Energy*. 44 (2019) 18744–18755. <https://doi.org/10.1016/j.ijhydene.2018.08.159>.
- [16] M. Izaki, K. Fukazawa, K. Sato, P.L. Khoo, M. Kobayashi, A. Takeuchi, K. Uesugi, Defect Structure and Photovoltaic Characteristics of Internally Stacked CuO/Cu₂O Photoactive Layer Prepared by Electrodeposition and Heating, *ACS Appl. Energy Mater.* 2 (2019) 4833–4840. <https://doi.org/10.1021/acsaem.9b00514>.
- [17] A.O. Musa, T. Akomolafe, M.J. Carter, Production of cuprous oxide, a solar cell material, by thermal oxidation and a study of its physical and electrical properties, *Solar Energy Materials and Solar Cells*. (1998) 12.
- [18] T. Minami, Y. Nishi, T. Miyata, J. Nomoto, High-Efficiency Oxide Solar Cells with ZnO/Cu₂O Heterojunction Fabricated on Thermally Oxidized Cu₂O Sheets, *Appl. Phys. Express*. 4 (2011) 062301. <https://doi.org/10.1143/APEX.4.062301>.
- [19] Y. Ilevskaya, R.L.Z. Hoyer, A. Sadhanala, K.P. Musselman, J.L. MacManus-Driscoll, Fabrication of ZnO/Cu₂O heterojunctions in atmospheric conditions: Improved interface quality and solar cell performance, *Solar Energy Materials and Solar Cells*. 135 (2015) 43–48. <https://doi.org/10.1016/j.solmat.2014.09.018>.
- [20] H. Zhu, J. Zhang, C. Li, F. Pan, T. Wang, B. Huang, Cu₂O thin films deposited by reactive direct current magnetron sputtering, *Thin Solid Films*. 517 (2009) 5700–5704. <https://doi.org/10.1016/j.tsf.2009.02.127>.
- [21] S. Dolai, S. Das, S. Hussain, R. Bhar, A.K. Pal, Cuprous oxide (Cu₂O) thin films prepared by reactive d.c. sputtering technique, *Vacuum*. 141 (2017) 296–306. <https://doi.org/10.1016/j.vacuum.2017.04.033>.
- [22] C. de Melo, M. Jullien, Y. Battie, A. En Naciri, J. Ghanbaja, F. Montaigne, J.-F. Pierson, F. Rigoni, N. Almqvist, A. Vomiero, S. Migot, F. Mücklich, D. Horwat, Semi-Transparent p-Cu₂O/n-ZnO Nanoscale-Film Heterojunctions for Photodetection and Photovoltaic Applications, *ACS Appl. Nano Mater.* 2 (2019) 4358–4366. <https://doi.org/10.1021/acsanm.9b00808>.

- [23] S.W. Lee, Y.S. Lee, J. Heo, S.C. Siah, D. Chua, R.E. Brandt, S.B. Kim, J.P. Mailoa, T. Buonassisi, R.G. Gordon, Improved Cu₂O-Based Solar Cells Using Atomic Layer Deposition to Control the Cu Oxidation State at the p-n Junction, *Advanced Energy Materials*. 4 (2014) 1301916. <https://doi.org/10.1002/aenm.201301916>.
- [24] A. Sekkat, V.H. Nguyen, C.A. Masse de La Huerta, L. Rapenne, D. Bellet, A. Kaminski-Cachopo, G. Chichignoud, D. Muñoz-Rojas, Open-air printing of Cu₂O thin films with high hole mobility for semitransparent solar harvesters, *Commun Mater*. 2 (2021) 78. <https://doi.org/10.1038/s43246-021-00181-8>.
- [25] Y.S. Lee, M.T. Winkler, S.C. Siah, R. Brandt, T. Buonassisi, Hall mobility of cuprous oxide thin films deposited by reactive direct-current magnetron sputtering, *Appl. Phys. Lett.* 98 (2011) 192115. <https://doi.org/10.1063/1.3589810>.
- [26] Chen Aiping, Hua Long, Xiangcheng Li, Yuhua Li, Guang Yang*, Peixiang Lu, Controlled growth and characteristics of single-phase Cu₂O and CuO films by pulsed laser deposition, *Vacuum*. 83 (2009) 927–930. <https://doi.org/10.1016/j.vacuum.2008.10.003>.
- [27] M. Pustan, C. Birleanu, V. Merie, L. Zarbo, S. Garabagiu, D. Marconi, Effect of deposition oxygen pressure on the properties of cuprous oxide thin films, *IOP Conf. Ser.: Mater. Sci. Eng.* 724 (2020) 012052. <https://doi.org/10.1088/1757-899X/724/1/012052>.
- [28] S.F.U. Farhad, D. Cherns, J.A. Smith, N.A. Fox, D.J. Fermín, Pulsed laser deposition of single phase n- and p-type Cu₂O thin films with low resistivity, *Materials & Design*. 193 (2020) 108848. <https://doi.org/10.1016/j.matdes.2020.108848>.
- [29] M.F. Jawad, R.A. Ismail, K.Z. Yahea, Preparation of nanocrystalline Cu₂O thin film by pulsed laser deposition, *J Mater Sci: Mater Electron*. 22 (2011) 1244–1247. <https://doi.org/10.1007/s10854-011-0294-0>.
- [30] X. Liu, M. Xu, X. Zhang, W. Wang, X. Feng, A. Song, Pulsed-laser-deposited, single-crystalline Cu₂O films with low resistivity achieved through manipulating the oxygen pressure, *Applied Surface Science*. 435 (2018) 305–311. <https://doi.org/10.1016/j.apsusc.2017.11.119>.
- [31] S.H. Wee, P.-S. Huang, J.-K. Lee, A. Goyal, Heteroepitaxial Cu₂O thin film solar cell on metallic substrates, *Sci Rep*. 5 (2015) 16272. <https://doi.org/10.1038/srep16272>.
- [32] K. Wang, W. Gao, H.W. Zheng, F.Z. Li, M.S. Zhu, G. Yang, G.T. Yue, Y.K. Liu, R.K. Zheng, Heteroepitaxial growth of Cu₂O films on Nb-SrTiO₃ substrates and their photovoltaic properties, *Ceramics International*. 43 (2017) 16232–16237. <https://doi.org/10.1016/j.ceramint.2017.08.205>.
- [33] S.B. Ogale, P.G. Bilurkar, N. Mate, S.M. Kanetkar, N. Parikh, B. Patnaik, Deposition of copper oxide thin films on different substrates by pulsed excimer laser ablation, *Journal of Applied Physics*. 72 (1992) 3765–3769. <https://doi.org/10.1063/1.352271>.
- [34] A. Subramaniyan, J.D. Perkins, R.P. O’Hayre, S. Lany, V. Stevanovic, D.S. Ginley, A. Zakutayev, Non-equilibrium deposition of phase pure Cu₂O thin films at reduced growth temperature, *APL Materials*. 2 (2014) 022105. <https://doi.org/10.1063/1.4865457>.
- [35] S.F.U. Farhad, R.F. Webster, D. Cherns, Electron microscopy and diffraction studies of pulsed laser deposited cuprous oxide thin films grown at low substrate temperatures, *Materialia*. 3 (2018) 230–238. <https://doi.org/10.1016/j.mtla.2018.08.032>.
- [36] M. Nolan, S.D. Elliott, The p-type conduction mechanism in Cu₂O: a first principles study, *Phys. Chem. Chem. Phys.* 8 (2006) 5350–5358. <https://doi.org/10.1039/B611969G>.
- [37] H. Raebiger, S. Lany, A. Zunger, Origins of the p-type nature and cation deficiency in Cu₂O and related materials, *Phys. Rev. B*. 76 (2007) 045209. <https://doi.org/10.1103/PhysRevB.76.045209>.
- [38] K. Han, M. Tao, Electrochemically deposited p–n homojunction cuprous oxide solar cells, *Solar Energy Materials and Solar Cells*. 93 (2009) 153–157. <https://doi.org/10.1016/j.solmat.2008.09.023>.

- [39] Z. Xi, H. Zeng, N. Liao, L. Shi, H. Huang, S. Guo, N. Wang, D. Jin, L. Wang, Study on the effect of annealing on the electrical properties of n-type cuprous oxide, *Thin Solid Films*. 520 (2012) 2708–2710. <https://doi.org/10.1016/j.tsf.2011.11.044>.
- [40] C. Zhu, M.J. Panzer, Synthesis of Zn:Cu₂O Thin Films Using a Single Step Electrodeposition for Photovoltaic Applications, *ACS Appl. Mater. Interfaces*. 7 (2015) 5624–5628. <https://doi.org/10.1021/acsami.5b00643>.
- [41] M. Xu, X. Liu, W. Xu, H. Xu, X. Hao, X. Feng, Low resistivity phase-pure n-type Cu₂O films realized via post-deposition nitrogen plasma treatment, *Journal of Alloys and Compounds*. 769 (2018) 484–489. <https://doi.org/10.1016/j.jallcom.2018.08.048>.
- [42] D.O. Scanlon, G.W. Watson, Undoped n-Type Cu₂O: Fact or Fiction?, *J. Phys. Chem. Lett.* 1 (2010) 2582–2585. <https://doi.org/10.1021/jz100962n>.
- [43] J.P. Stoquert, F. Pêcheux, Y. Hervé, H. Marchal, R. Stuck, P. Siffert, VRBS: A virtual RBS simulation tool for ion beam analysis, *Nuclear Instruments and Methods in Physics Research Section B: Beam Interactions with Materials and Atoms*. 136–138 (1998) 1152–1156. [https://doi.org/10.1016/S0168-583X\(97\)00807-0](https://doi.org/10.1016/S0168-583X(97)00807-0).
- [44] A. Sambri, M. Radovic', X. Wang, S. Amoruso, F.M. Granozio, R. Bruzese, Substrate heating effects on the propagation dynamics of laser produced plume during pulsed laser deposition of oxides, *Applied Surface Science*. 254 (2007) 790–793. <https://doi.org/10.1016/j.apsusc.2007.07.183>.
- [45] T. Armbruster, R.M. Danisi, eds., 1. The power of databases: The RRUFF project, in: *Highlights in Mineralogical Crystallography*, De Gruyter (O), 2015: pp. 1–30. <https://doi.org/10.1515/9783110417104-003>.
- [46] T. Sander, C.T. Reindl, M. Giar, B. Eifert, M. Heinemann, C. Heiliger, P.J. Klar, Correlation of intrinsic point defects and the Raman modes of cuprous oxide, *Phys. Rev. B*. 90 (2014) 045203. <https://doi.org/10.1103/PhysRevB.90.045203>.
- [47] A. Compaan, Surface damage effects on allowed and forbidden phonon raman scattering in cuprous oxide, *Solid State Communications*. 16 (1975) 293–296. [https://doi.org/10.1016/0038-1098\(75\)90171-4](https://doi.org/10.1016/0038-1098(75)90171-4).
- [48] A.L. Patterson, The Scherrer Formula for X-Ray Particle Size Determination, *Phys. Rev.* 56 (1939) 978–982. <https://doi.org/10.1103/PhysRev.56.978>.
- [49] A.R. Stokes, A.J.C. Wilson, The diffraction of X rays by distorted crystal aggregates - I, *Proceedings of the Physical Society*. 56 (1944) 174–181. <https://doi.org/10.1088/0959-5309/56/3/303>.
- [50] M. Ohring, *The Materials Science of Thin Solid Films*, (1992).
- [51] A.S. Reddy, S. Uthanna, P.S. Reddy, Properties of dc magnetron sputtered Cu₂O films prepared at different sputtering pressures, *Applied Surface Science*. 253 (2007) 5287–5292. <https://doi.org/10.1016/j.apsusc.2006.11.051>.
- [52] G.E. Jellison, F.A. Modine, Parameterization of the optical functions of amorphous materials in the interband region, *Applied Physics Letters*. 69 (1996) 371–373. <https://doi.org/10.1063/1.118064>.
- [53] T. Ito, T. Kawashima, H. Yamaguchi, T. Masumi, S. Adachi, Optical Properties of Cu₂O Studied by Spectroscopic Ellipsometry, *Journal of the Physical Society of Japan*. 67 (1998) 2125–2131. <https://doi.org/10.1143/JPSJ.67.2125>.
- [54] T. Ito, H. Yamaguchi, T. Masumi, S. Adachi, Optical Properties of CuO Studied by Spectroscopic Ellipsometry, *Journal of the Physical Society of Japan*. 67 (1998) 3304–3309. <https://doi.org/10.1143/JPSJ.67.3304>.
- [55] H. Rahal, R. Kihal, A.M. Affoune, S. Rahal, Electrodeposition and characterization of Cu₂O thin films using sodium thiosulfate as an additive for photovoltaic solar cells, *Chinese Journal of Chemical Engineering*. 26 (2018) 421–427. <https://doi.org/10.1016/j.cjche.2017.06.023>.

- [56] H. Matsumura, A. Fujii, T. Kitatani, Properties of High-Mobility Cu₂O Films Prepared by Thermal Oxidation of Cu at Low Temperatures, *Japanese Journal of Applied Physics*. 35 (1996) 5631–5636. <https://doi.org/10.1143/jjap.35.5631>.
- [57] W.-Y. Yang, S.-W. Rhee, Effect of electrode material on the resistance switching of Cu₂O film, *Applied Physics Letters*. 91 (2007) 232907. <https://doi.org/10.1063/1.2822403>.
- [58] J. Deuermeier, H. Liu, L. Rapenne, T. Calmeiro, G. Renou, R. Martins, D. Muñoz-Rojas, E. Fortunato, Visualization of nanocrystalline CuO in the grain boundaries of Cu₂O thin films and effect on band bending and film resistivity, *APL Materials*. 6 (2018) 096103. <https://doi.org/10.1063/1.5042046>.
- [59] V.T. Agekyan, Spectroscopic properties of semiconductor crystals with direct forbidden energy gap, *Phys. Stat. Sol. (a)*. 43 (1977) 11–42. <https://doi.org/10.1002/pssa.2210430102>.
- [60] Y. Wang, S. Lany, J. Ghanbaja, Y. Fagot-Revurat, Y.P. Chen, F. Soldera, D. Horwat, F. Mücklich, J.F. Pierson, Electronic structures of Cu₂O, Cu₄O₃ and CuO: A joint experimental and theoretical study, *Phys. Rev. B*. 94 (2016) 245418. <https://doi.org/10.1103/PhysRevB.94.245418>.
- [61] L. Xu, G. Zheng, S. Pei, J. Wang, Investigation of optical bandgap variation and photoluminescence behavior in nanocrystalline CuO thin films, *Optik*. 158 (2018) 382–390. <https://doi.org/10.1016/j.ijleo.2017.12.138>.
- [62] A. Chen, G. Yang, H. Long, F. Li, Y. Li, P. Lu, Nonlinear optical properties of laser deposited CuO thin films, *Thin Solid Films*. 517 (2009) 4277–4280. <https://doi.org/10.1016/j.tsf.2008.11.139>.
- [63] F.-Y. Ran, H. Hiramatsu, H. Hosono, T. Kamiya, M. Taniguti, Detection of dead layers and defects in polycrystalline Cu₂O thin-film transistors by x-ray reflectivity and photoresponse spectroscopy analyses, *Journal of Vacuum Science & Technology B, Nanotechnology and Microelectronics: Materials, Processing, Measurement, and Phenomena*. 33 (2015) 051211. <https://doi.org/10.1116/1.4929445>.
- [64] L. Zhang, L. McMillon, J. McNatt, Gas-dependent bandgap and electrical conductivity of Cu₂O thin films, *Solar Energy Materials and Solar Cells*. 108 (2013) 230–234. <https://doi.org/10.1016/j.solmat.2012.05.010>.
- [65] T. Minami, Y. Nishi, T. Miyata, Impact of incorporating sodium into polycrystalline p-type Cu₂O for heterojunction solar cell applications, *Appl. Phys. Lett.* 105 (2014) 212104. <https://doi.org/10.1063/1.4902879>.
- [66] K. Mizuno, M. Izaki, K. Murase, T. Shinagawa, M. Chigane, M. Inaba, A. Tasaka, Y. Awakura, Structural and Electrical Characterizations of Electrodeposited p-Type Semiconductor Cu₂O Films, *Journal of The Electrochemical Society*. 152 (2005) C179–C182. <https://doi.org/10.1149/1.1862478>.
- [67] Z.Q. Yu, C.M. Wang, M.H. Engelhard, P. Nachimuthu, D.E. McCready, I.V. Lyubnitsky, S. Thevuthasan, Epitaxial growth and microstructure of Cu₂O nanoparticle/thin films on SrTiO₃(100), *Nanotechnology*. 18 (2007) 115601. <https://doi.org/10.1088/0957-4484/18/11/115601>.
- [68] C.Y. Lam, K.H. Wong, Characteristics of heteroepitaxial Cu₂-xMnxO/Nb-SrTiO₃ p-n junction, *Journal of Non-Crystalline Solids*. 354 (2008) 4262–4266. <https://doi.org/10.1016/j.jnoncrysol.2008.06.097>.
- [69] P. Cendula, M.T. Mayer, J. Luo, M. Grätzel, Elucidation of photovoltage origin and charge transport in Cu₂O heterojunctions for solar energy conversion, *Sustainable Energy Fuels*. 3 (2019) 2633–2641. <https://doi.org/10.1039/C9SE00385A>.
- [70] J. Kaur, O. Bethge, R.A. Wibowo, N. Bansal, M. Bauch, R. Hamid, E. Bertagnolli, T. Dimopoulos, All-oxide solar cells based on electrodeposited Cu₂O absorber and atomic layer deposited ZnMgO on precious-metal-free electrode, *Solar Energy Materials and Solar Cells*. 161 (2017) 449–459. <https://doi.org/10.1016/j.solmat.2016.12.017>.